

Contents lists available at ScienceDirect

Solar Energy

journal homepage: www.elsevier.com/locate/solener



Study on characteristics of interfacial microstructure and electrical current mechanism in Sn-xZn/Al photovoltaic modules



Chia-Wei Lin, Fei-Yi Hung*, Truan-Sheng Lui, Di-Jung Huang

Department of Materials Science and Engineering, National Cheng Kung University, Tainan 701, Taiwan

ARTICLE INFO

Keywords:
Photovoltaic (PV) aluminum ribbon
Sn-Zn solder
PV module
Bias aging

ABSTRACT

The microstructural characteristics, bonding force and bulk resistance of photovoltaic (PV) aluminum modules made with three hypereutectic solder alloys, namely Sn-30Zn, Sn-50Zn and Sn-70Zn, were investigated. In the dipping step, the mechanism of bonding between pure aluminum ribbons and Sn-xZn solder alloys is via the Sn-xZn solder liquid phase penetrating into aluminum grain boundaries rather than forming intermetallic compound at the interface. After reflow for connecting PV aluminum ribbon and silicon substrate with Ag paste, an AgZn₃ layer, whose thickness increases with increasing reflow time, formed at the solder/Ag interface. After bias aging, the Ag paste was consumed, the thickness of AgZn₃ significantly increased and the bulk resistance increased. The bulk resistance of the modules with "Ag direction" (electrons move from Al to Ag) is slightly higher than that of modules with "Al direction" (electrons move from Ag to Al) due to more formation of AgZn₃, which decreases the cross-section area of electrical current and increases the path of electrical current. Sn-50Zn/Al PV modules have good stability and high conductivity, and are competitive with PV modules made with copper ribbons.

1. Introduction

Photovoltaic (PV) ribbons are applied in solar cell modules for connecting the solar silicon substrate and collecting photo-generated current. A PV ribbon is a metallic thin ribbon with a solder dipping that has good weldability and conductivity. A silver paste is used to be the electrode and for connecting a PV ribbon to the silicon substrate as it improves bonding ability. Nowadays, commercial PV ribbons still use Sn-Pb alloy solders such as Sn-36Pb-2Ag and Sn-37Pb because of their good weldability and mechanical properties (Lathrop and Pfluke, 2011). However, these solders composed with Pb are harmful to the environment and human health (Miric and Grusd, 1998; Trumble, 1998). Thus, lead-free solders such as Sn-Ag, Sn-Zn and Sn-Ag-Cu have been developed in recent years. Moreover, previous studies (Tian et al., 2011; Frear et al., 1994) have found that high-resistance intermetallic compounds (IMCs) such as Ag_3Sn and Cu_6Sn_5 are formed in Sn-Ag and Sn-Ag-Cu series alloys, degrading conversion efficiency (Nieland et al., 2007). In addition, adding Ag increases the cost of PV ribbons. Hence, Sn-Zn solder alloys are used in the present study.

Sn-Zn solder has been studied in some previous researches (Gayle et al., 2001; Wei et al., 2007; Lan et al., 2011). For general lead-free solder, Sn-Zn alloys have the lowest cost. Their eutectic composition is Sn-9Zn (in wt.%) and their melting point and mechanical properties are

Notably, 1050 pure aluminum ribbons are used in this research instead of Cu ribbon, which is commonly used in PV modules. Although the conductivity of aluminum is lower than that of copper, the cost of aluminum is much lower than that of copper (about four fold) and IMCs do not form with Al (according to the Al-Sn phase diagram (Humpston, 1993). Therefore, a pure aluminum ribbon has potential for applying in solar photovoltaic modules.

Based on the above mentioned reasons, hypereutectic Sn-Zn solder alloys and 1050 pure aluminum ribbons are adopted for fabricating PV modules in this study. Bonding reliability, microstructural characteristics and conductivity are evaluated and analyzed to determine the applicability of PV modules fabricated with Sn-xZn (x = 30, 50, and 70 wt%) solder alloys and pure aluminum ribbons.

E-mail address: fyhung@mail.ncku.edu.tw (F.-Y. Hung).

similar to those of Sn-Pb solder alloys. As the composition is hypereutectic, a needle-like Zn-rich phase and Sn-Zn eutectic phases form (Lan et al., 2011). The electrical resistance of Zn (0.059 $\mu\Omega\text{-m}$) is lower than that of Sn (0.115 $\mu\Omega\text{-m}$), and thus the Zn-rich phase is a better path for electrical current. Therefore, the Sn-Zn alloys with hypereutectic compositions are used in this study for enhancing the primary Zn-rich phase content and improving conductivity.

^{*} Corresponding author.

C.-W. Lin et al. Solar Energy 170 (2018) 840–848

Table 1Chemical composition of 1050 aluminum ribbon.

Element	Si	Fe	Zn	Ti	V	Al
wt. %	0.09	0.21	0.01	0.02	0.01	Bal.

Table 2
Chemical composition of Sn-xZn solder alloys (wt. %).

	Sn	Zn
Sn-30Zn	72.6	27.4
Sn-50Zn	50.3	49.7
Sn-70Zn	30.0	70.0



Fig. 1. Illustration of PV module.

2. Materials and methods

The chemical composition of 1050 aluminum ribbon is shown in Table 1. Sn-30Zn, Sn-50Zn, and Sn-70Zn, all of which have a hypereutectic composition, were prepared and adopted. Their accurate compositions are shown in Table 2.

The three Sn-Zn solder alloys were heated to 450 °C for melting. The aluminum ribbons were machined into specimens with the dimensions of 30 mm (length) \times 2 mm (width) \times 0.3 mm (thickness) and were soaked in acetone for ultrasonic cleaning. Then, the Al ribbons were dipped into melted Sn-Zn liquid (with flux, Goot BS-10) for 5 s The Al ribbons were cladded in Sn-Zn alloys to finish the fabrication of PV ribbons. Finally, the PV ribbons were reflowed onto an Ag paste (with flux) on a silicon substrate at 340 °C for manufacturing PV modules as shown in Fig. 1.

Fig. 2 shows the connection of the PV aluminum ribbons and the silicon substrate. The length of an aluminum ribbon was 20 mm. The reflow durations were set as 10, 20 and 30 s. The dimensions of the reflowed specimens are shown in Fig. 2(b). The reflowed specimens are also the specimens using in the peeling force test and in the bias aging. Part of PV ribbon (about 10 mm) uncovered by solder alloy is prepared for being clamped by the crosshead in the peeling force test and being connected with the DC power supply.

The microstructure of the PV ribbons and reflowed specimens was observed using optical microscopy (OM) and scanning electron microscopy (SEM). The microstructural characteristics and interfacial microstructure were analyzed using SEM, energy-dispersive X-ray spectroscopy (EDS), and an electron probe micro-analyzer (EPMA). In order to quantify the ratio of the Zn-rich phase in the dipping layer of PV

ribbons, the thickness dissimilarity of IMCs and the Ag paste layer of asfabricated PV ribbons and reflowed PV ribbons were calculated using the software "ImageJ". Data are presented as the average of at least three samples.

The peeling force test shown in Fig. 3 was applied to evaluate the bonding strength between PV ribbon and substrate after reflowing. At first, the 10 mm-length naked aluminum ribbon was clamped by the crosshead. Then, the peeling force test started and the bonding layer started to be tore. The test carried on until the bonding layer was totally destroyed and the peeling force was recorded to be the bonding strength. This method is often applied to solar cells for estimating bonding reliability. The basic standard bonding force is 100 gf (Chen et al., 2015); that is, the peeling force should be larger than 100gf at least. The tensile force was perpendicular to the bonding surface of the PV ribbons. The peeling velocity was set as 20 mm/min. The Sn-xZn PV module with the highest peeling force was used in the subsequent bias aging test.

In the bias aging test, a DC power supply provided a current for the PV modules at room temperature. Two electrical current directions were used, as shown in Fig. 4, since they both exist in PV modules, as shown in Fig. 2(a). When the positive terminal of the DC power supply was connected to an Ag paste electrode on the Si substrate and the negative terminal was connected to the pure Al ribbon, this created a flow direction defined as the "Al direction" (electrons move from Al to Ag, as shown in Fig. 4(a)). The opposite flow direction is defined as the "Ag direction" (electrons move from Al to Ag, as shown in Fig. 4(b)). The effects of electrical current directions on bulk resistance and microstructure were investigated and compared with each other.

The current-voltage curve (I-V curve) method was applied to evaluate bulk resistance (Alford et al., 2009; Hung et al., 2011). The maximum current was set at 16 A (70% of the fusing current); the current was increased at a rate of 0.5 A/s. The duration of the electrical current test (bias aging) was set as 72 h. The bulk resistance was evaluated before and after bias aging. In addition, the highest temperature of PV ribbons in the bias aging with above condition is about 80 °C, which is not effective for increasing the thickness of IMCs.

The influence of bias aging for 72 h on microstructural evolution and interface characteristics was observed using OM, SEM, EDS, and EPMA.

3. Results and discussion

3.1. Microstructure characteristics and bonding mechanism of Sn-xZn PV Al ribbons

Fig. 5(a)–(c) show the microstructures of Sn-30Zn, Sn-50Zn, and Sn-70Zn, respectively. The black and coarse needle-like phases are the primary Zn-rich phase. The block-like phase, also a Zn-rich phase, increases with increasing Zn content. The eutectic phase, which is composed of the fine needle-like Zn-rich phase and β -Sn, exists in the matrix. A layer of the Zn-rich phase appears at the interface between Sn-Zn

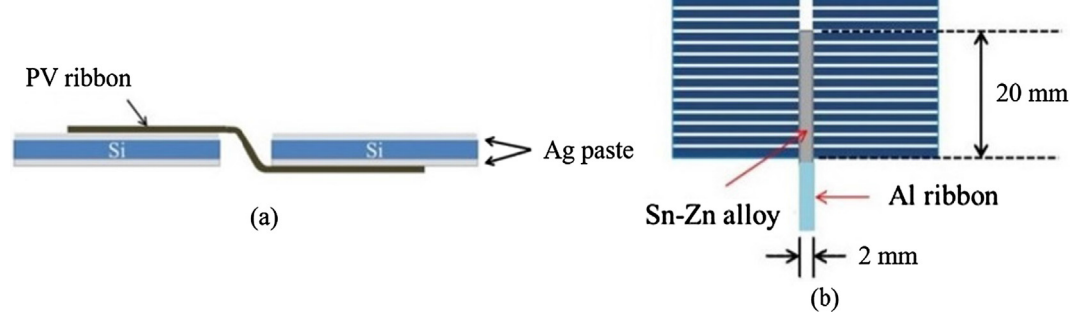


Fig. 2. (a) Illustration of connection of PV ribbon and silicon substrate and (b) dimensions of reflowed specimen.

Download English Version:

https://daneshyari.com/en/article/7935130

Download Persian Version:

https://daneshyari.com/article/7935130

<u>Daneshyari.com</u>